Electronic Supplementary Information

Insights into enhanced photoelectrochemical performance of hydrothermally controlled Hematite Nanostructures for Proficient Solar Water Oxidation

Jin Woo Park[a], Arunprabaharan Subramanian[a], Mahadeo A. Mahadik[a], Su Yong Lee[b], Sun Hee Choi[b] and Jum Suk Jang[a]*

[a.]Division of Biotechnology, Safety, Environment and Life Science Institute, College of Environmental and Bioresource Sciences, Chonbuk National University, Iksan 54596, Korea.

[b.]Pohang Accelerator Laboratory (PAL), Pohang University of Science and Technology (POSTECH), Pohang 37673, Republic of Korea

*Corresponding authors. Tel.: +82 63 850 0846; fax: +82 63 850 0834.

E-mail address: jangjs75@jbnu.ac.kr

Table S1 Average diameter and length of before (β-FeOOH photoanodes) and after (α-Fe_2O_3 photoanodes) high temperature annealing for FH1 (a), FH3, (b), FH6 (c), FH9 (d), FH12 (e), FH18 (f), FH1Q (a)*, FH3Q, (b)*, FH6Q (c)*, FH9Q (d)*, FH12Q (e)* and FH18Q (f)*, respectively

	Before high temperature annealing						After high temperature annealing					
sample	(a)	(b)	(c)	(d)	(e)	(f)	(a)*	(b)*	(c)*	(d)*	(e)*	(f)*
Average Diameter (nm)	55	78	96	101	113	130	67	98	110	176	195	222
Average Length (nm)	308	390	500	533	560	684	174	349	466	452	520	573

Table S2 Calculated crystalline size from XRD patterns at (110) plane of Fe_2O_3 photoanodes synthesized at (a) FH1Q, (b) FH3Q, (c) FH6Q, (d) FH9Q, (e) FH12Q, and (f) FH18Q, respectively.

Sample/Crystallite size	D_{110} (nm)
(a)	68.8
(b)	86.1
(c)	81.6
(d)	81.9
(e)	85.1
(f)	83.7

Table S3 Atomic concentration of Fe_2O_3 photoanodes obtained from XPS spectra for FH1Q (a), FH3Q, (b), FH6Q (c), FH9Q (d), FH12Q (e) and, FH18Q (f), respectively.

Samples/Atomic concentrations	Fe (Atomic %)	O (Atomic %)	Sn (Atomic %)
(a)	36.98	61.53	1.48
(b)	37.91	61.37	0.71
(c)	37.64	61.99	0.36
(d)	37.07	62.55	0.38
(e)	36.13	64.48	0.37
(f)	35.34	64.42	0.24

Table S4 Structural parameters calculated from Fe K-edge EXAFS fits for Fe_2O_3 photoanodes synthesized for FH1Q (a), FH3Q, (b), FH6Q (c), FH9Q (d), FH12Q (e) and FH18Q (f), respectively

Samples/ Structural parameters	R_1 (Å)[a]	R_2 (Å)[b]	σ^2 (Å^2)[c]	R-factor[d]	Fe-O[a,b]
(a)	1.908	2.075	0.0009	0.0232	
(b)	1.931	2.100	0.0026	0.0050	
(c)	1.943	2.113	0.0026	0.0149	
(d)	1.948	2.118	0.0022	0.0029	
(e)	1.927	2.096	0.0036	0.0308	
(f)	1.936	2.106	0.0037	0.0175	

bond distance (uncertainty < 0.007), [c] Debye-Waller factor(indicator of the structural disorder, uncertainty < 0.0008), [d] a sum-of-squares measure of the fractional misfit.

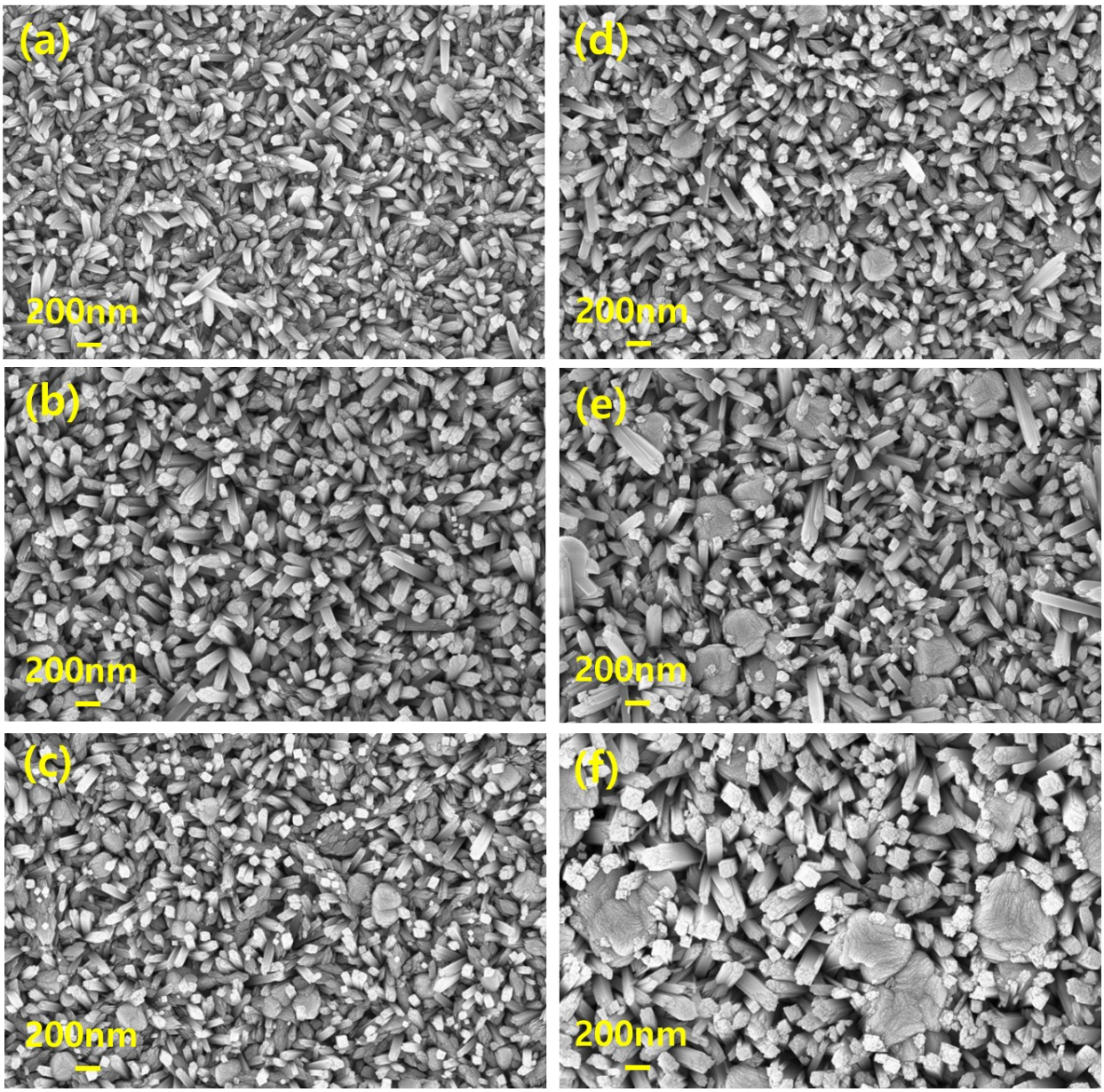

Figure S1 FESEM top view images of β-FeOOH photoanodes synthesized for (a) FH1, (b) FH3, (c) FH6, (d) FH9, (e) FH12, and (f) FH18, respectively.

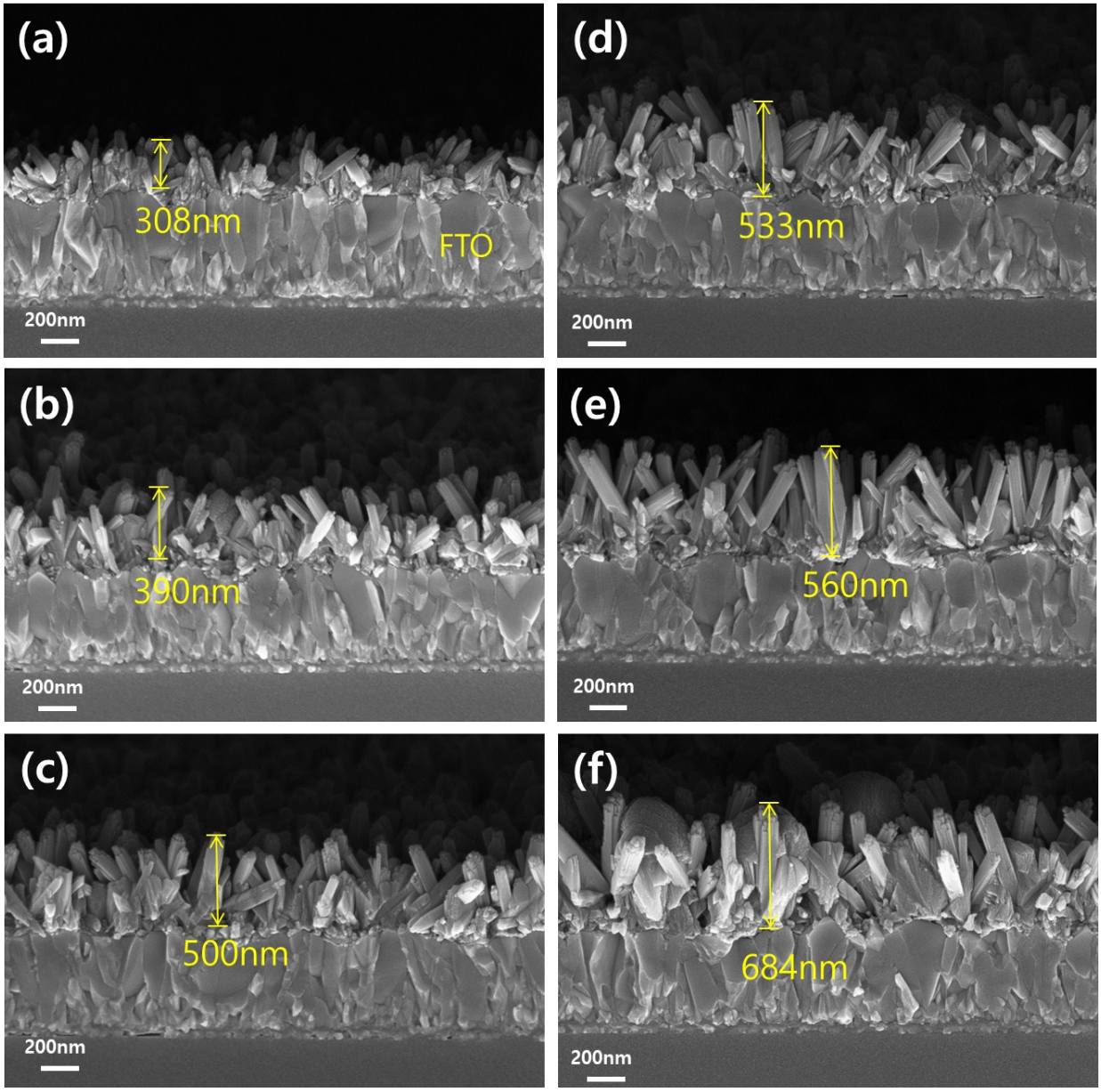

Figure S2 FESEM cross-sectional images of β-FeOOH photoanodes synthesized for (a) FH1, (b) FH3, (c) FH6, (d) FH9, (e) FH12, and (f) FH18, respectively.

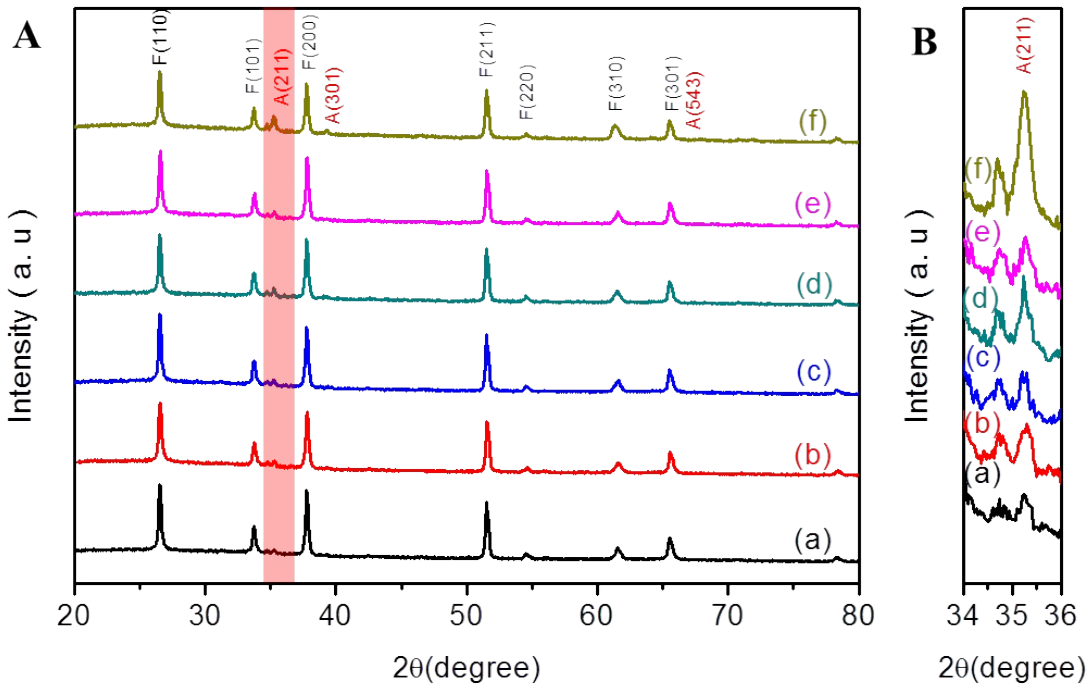

Figure S3 (A) XRD patterns of β-FeOOH photoanodes synthesized for (a) FH1, (b) FH3, (c) FH6, (d) FH9, (e) FH12, and (f) FH18, respectively, (B) Magnified view of the XRD profiles

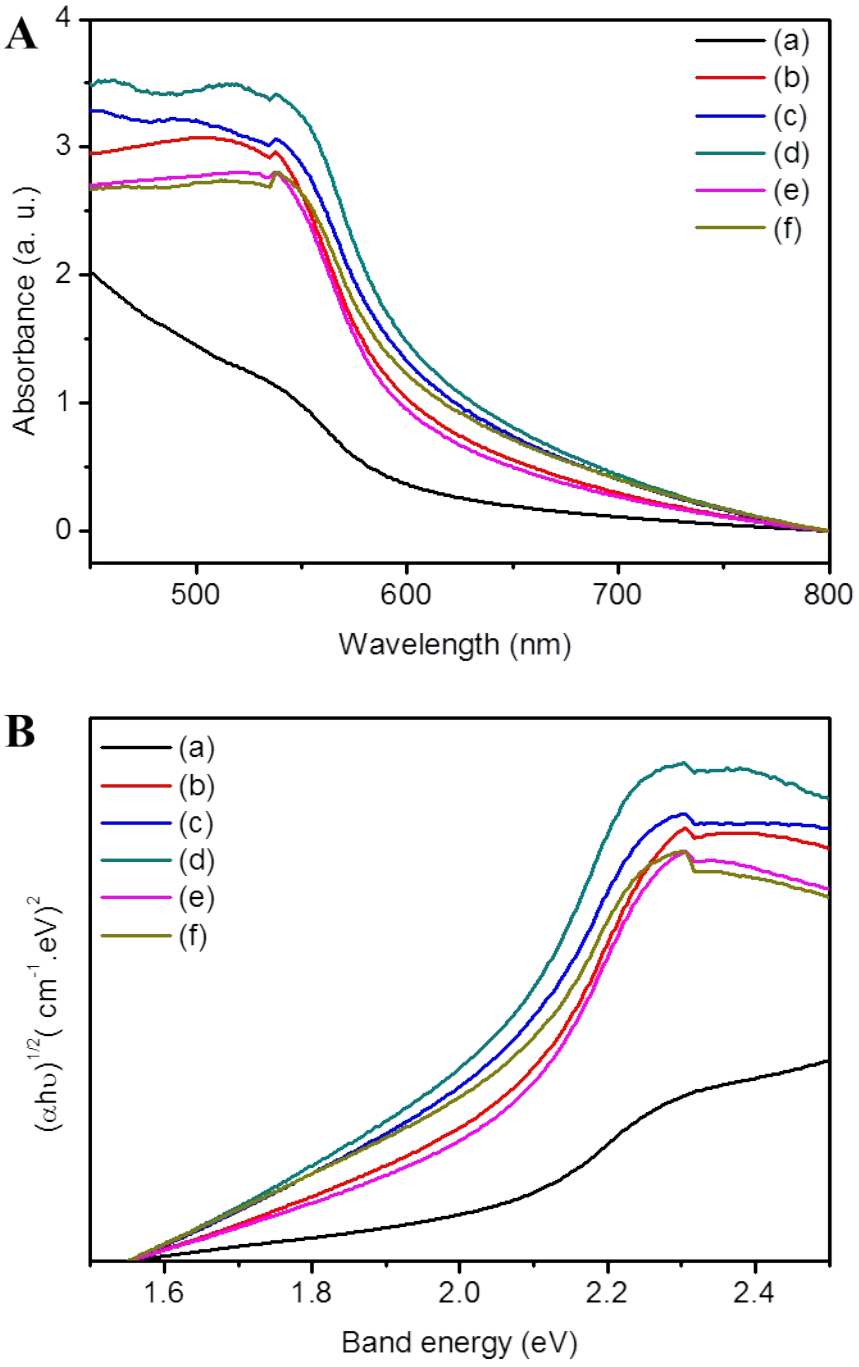

Figure S4 (A) UV–vis absorbance spectra and (B) Tauc plots of α-Fe_2O_3 photoanodes synthesized at FH1Q (a), FH3Q, (b), FH6Q (c), FH9Q (d), FH12Q (e) and FH18Q (f), respectively.`

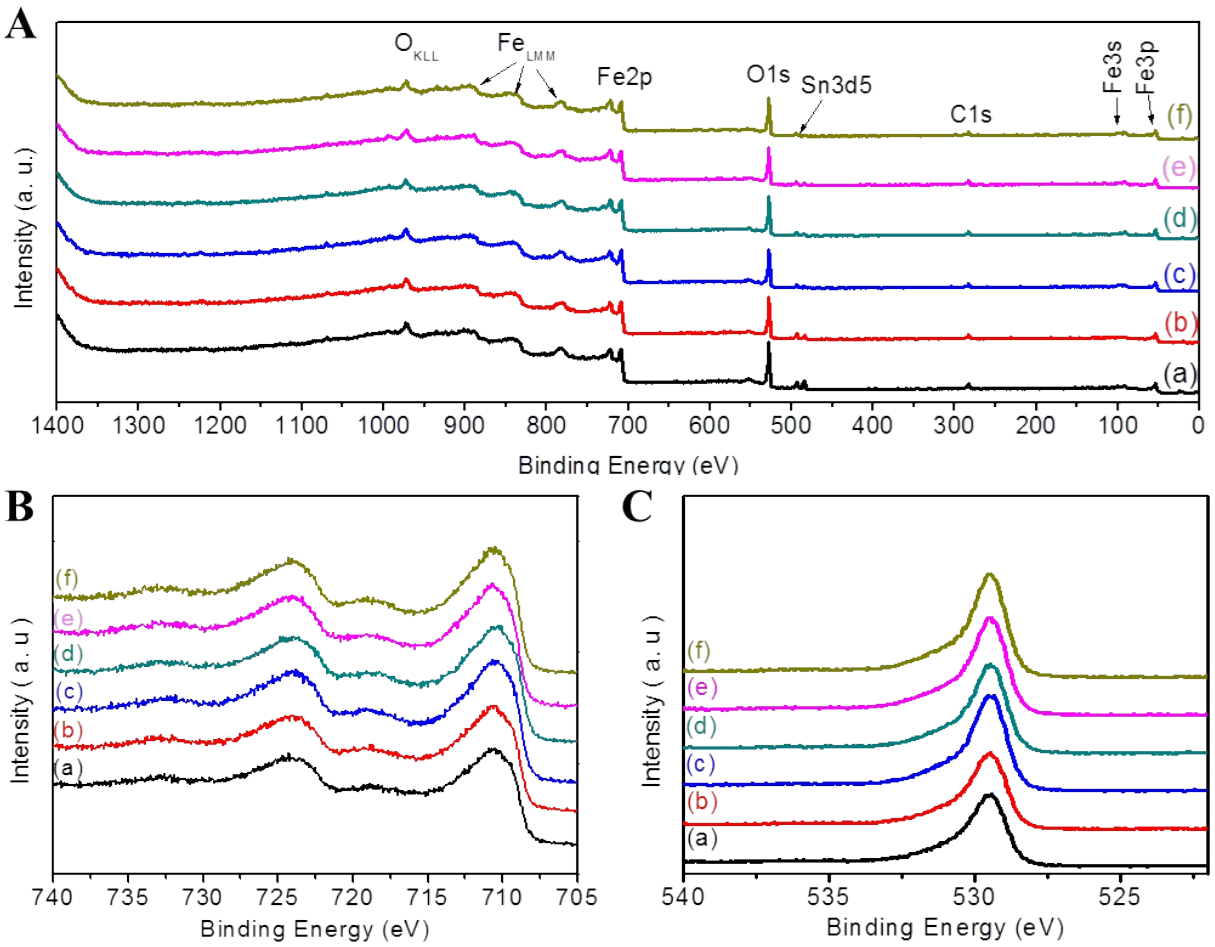

Figure S5 A) XPS survey scan spectra of hydrothermally prepared α-Fe_2O_3 photoanodes at FH1Q (a), FH3Q, (b), FH6Q (c), FH9Q (d), FH12Q (e) and FH18Q (f), B) High resolution XPS narrow scan of O 1s, C) Fe 2p, respectively.

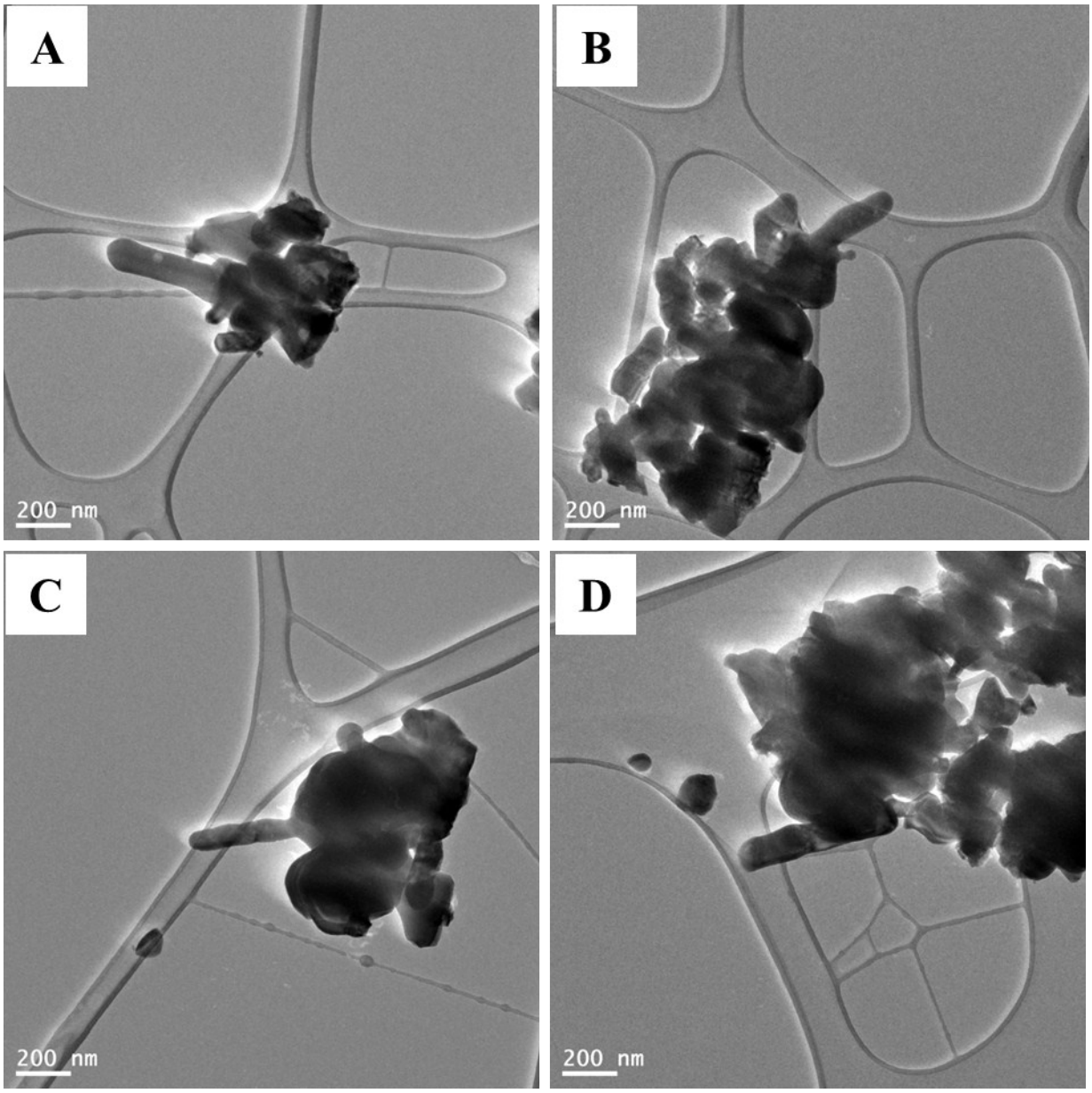

Figure S6 Low magnification TEM image of Fe_2O_3 photoanodes synthesized at (A-B) FH3Q, and (C-D) FH18Q, respectively.

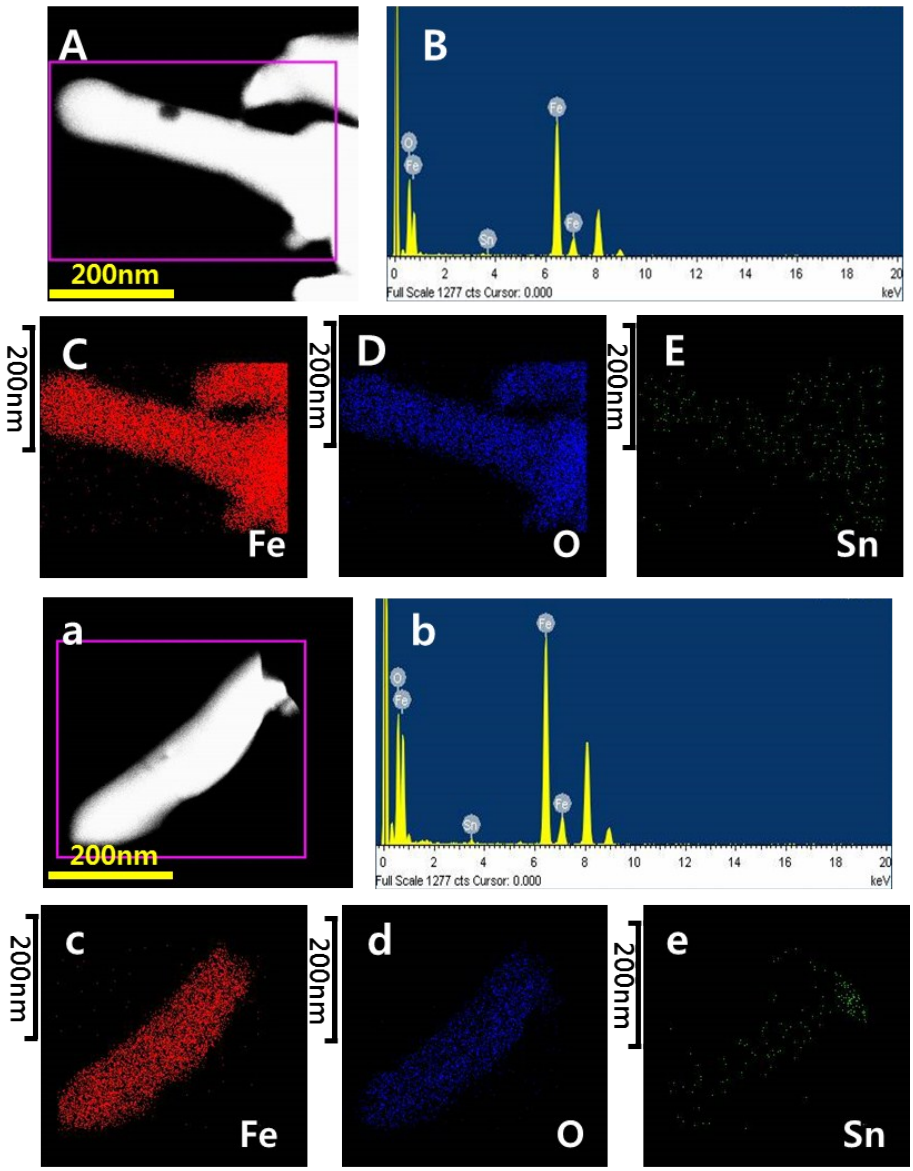

Figure S7 (A) TEM image of FH3Q, (B) EDS spectra and (C-E) corresponding EDS mapping of the selected TEM image with corresponding elemental mapping images for Fe, O and Sn, respectively, (a) TEM image of FH18Q nanorods, (b) EDX spectra and (c-e) elemental mapping images of single nanorod of FH18Q electrode.